



Lithological discrimination and mineralogical mapping using ASTER remote sensing data in the east-central Jebilet region, Morocco

Hayat El Khounaijri^{1*}, Ahmed Algouti¹, Abdellah Algouti¹, Mohamed Essemani¹, Fatiha Hadach², Soukaina Baid¹, Salma Ezzahzi¹, Salma Kabili¹, Saloua Agli¹, Naji Jdaba²

¹Department of Geology, Faculty of Sciences Semlalia, Cadi Ayyad University, Marrakesh, Morocco ²Department of Geology, Faculty of Sciences, Ibno Zohr University, Agadir, Morocco * corresponding author; e-mail: hayat.elkhounaijri2@gmail.com

Abstract

This study evaluates the effectiveness of ASTER (Advanced Spaceborne Thermal Emission and Reflection Radiometer) satellite data for lithological discrimination and mineralogical mapping in the east-central Jebilet region, Morocco. ASTER data offer considerable potential for detecting spectral signatures of mineral zones and determining their composition. The main objective is to apply image processing techniques, such as band ratios (BR), principal component analysis (PCA) and minimum noise fraction (MNF), in order to identify and map characteristic minerals in the region. The application of various band ratios effectively mapped the distribution of key minerals and alteration zones in the study area. The band ratio (band7/band5) was used to identify kaolinite, while the ratio (band4+band6)/band5 highlighted the presence of a mineral group constisting of alunite, kaolinite and pyrophyllite. The ratio (band7+band9)/ band8 revealed a set of a carbonate mineral, chlorite and epidote, whereas endoskarns composed of epidote, chlorite and amphibole were mapped using the ratio (band6+band9)/(band7+band8). The ratio (band5+band7)/band6 characterised phyllic alteration by detecting phyllosilicate minerals such as sericite, muscovite or illite. Phengite was mapped using the band5/band6 ratio. The distribution of these minerals was closely linked to the lithological variability of previously mapped geological units, highlighting the relevance and effectiveness of band ratios for geological mapping using remote sensing. The PCA and MNF components with the highest eigenvalues significantly improved lithological discrimination by reducing noise and refining the delineation of mineral zones. The results obtained have enabled the creation of a detailed map of mineral distribution, highlighting the alteration zones and lithological formations in the eastern Jebilet region of Morocco.time-consuming, yet inexpensive method that can be applied to other areas, especially those that are difficult to reach.

Keywords: GIS, ASTER, central Jebilet, lithological discrimination, mineralogical mapping

1. Introduction

Lithological and mineralogical mapping is essential for various geological applications, including mining exploration, natural resource management and environmental monitoring (Brimhall et al., 2005). Traditionally, such maps are produced

using geological field surveys, which, although accurate, are often costly and time consuming, especially in large and inaccessible areas.

With technological advancements, satellite remote sensing has become an indispensable tool for geological mapping. Multispectral and hyperspectral sensors enable detailed analysis of earth's sur-

face characteristics by capturing data in multiple spectral bands (Chen et al., 2024). Among these sensors, the Advanced Spaceborne Thermal Emission and Reflection Radiometer (ASTER) stands out for its ability to acquire data in 14 spectral bands, covering the visible, near-infrared, mid-infrared and thermal infrared regions (Laurent, 2019). While AS-TER is widely used for lithological discrimination due to its unique combination of 14 spectral bands, other satellites such as Sentinel and hyperspectral imaging satellites like PRISMA and EnMAP offer additional capabilities. Sentinel provides high spatial resolution and frequent revisit times, while hyperspectral sensors like PRISMA and EnMAP deliver detailed spectral information, enabling even more precise mineralogical and lithological analyses (Guanter et al., 2015).

The east-central Jebilet region in Morocco is renowned for its geological complexity, including metallic deposits and Palaeozoic formations (Bouloton et al., 2019). This diversity makes the discrimination of lithological units challenging with traditional methods, especially in highly altered areas where geochemical signatures are obscured. Furthermore, traditional geological mapping methods face limitations in such environments due to the impacts of hydrothermal alteration and variability of geological units (Abdelouhed et al., 2021).

The present study aims to evaluate the effectiveness of ASTER data for lithological discrimination and mineralogical mapping in the east-central Jebilet region. Although remote sensing techniques have been widely applied in various geological contexts, a study by Abdelouahed et al. (2021) focused on the same study area, but specifically concentrated on hydrothermal alteration zones. In contrast, the present research focuses on lithological discrimination and broader mineralogical mapping of the area. Specific objectives include the use of band ratios, principal component analysis (PCA) and minimum noise fraction (MNF), which have proved effective in identifying specific lithologies such as carbonate formations, shales and intrusive rocks. In addition, remote sensing results will be compared with geological field data and the Huvelin (1977) geological map (1:100,000) to validate the accuracy of the methods used.

2. Geographical location and geological framework of the study area

The eastern Jebilet are located in central Morocco, about 30 km north of the city of Marrakech, and are part of the Hercynian chain of the Western High Atlas (Michard, 1976). This region belongs to the Ancient Massif domain, a Precambrian and Palaeozoic zone that has undergone several tectonic phases, notably Hercynian orogeny, characterised by folding and magmatic intrusions (Michard, 1976).

The Jebilet consist mainly of Palaeozoic metasedimentary rocks (pelites, sandstones and limestones) and volcanic formations. There are also magmatic

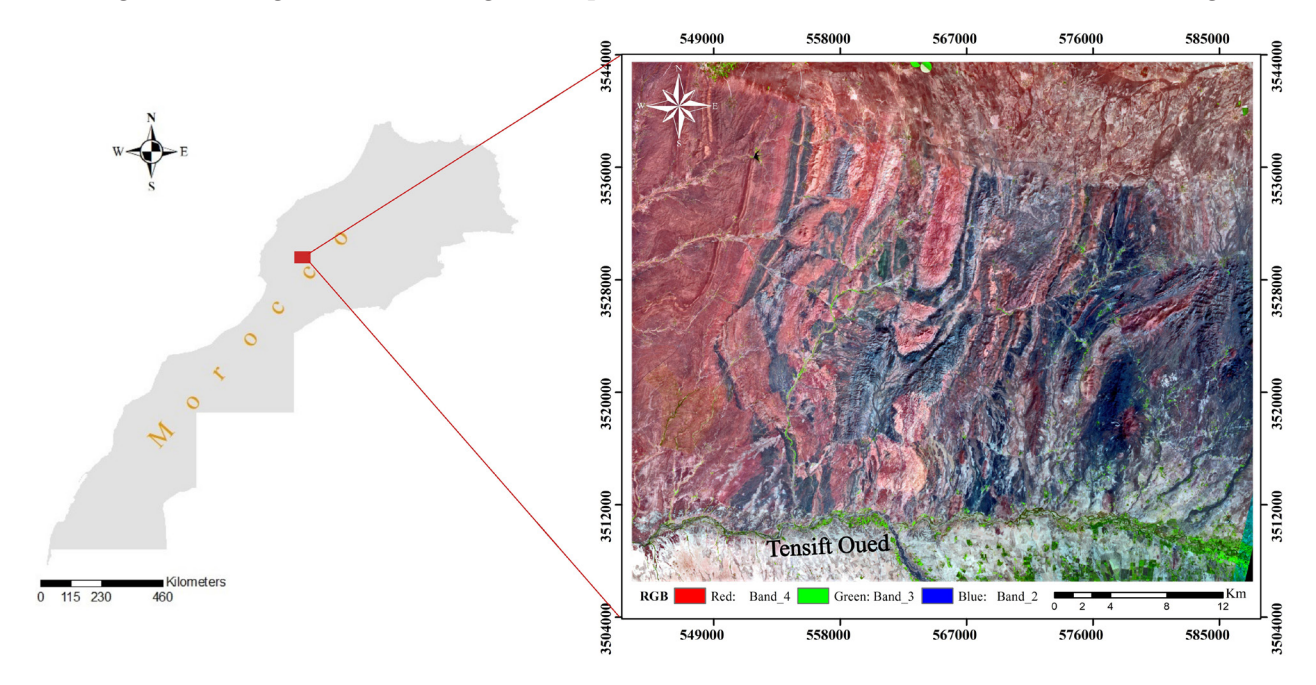


Fig. 1. Geographical location of the study area displayed with an ASTER RGB image (4-3-2) of the east-central Jebilet region, Morocco.

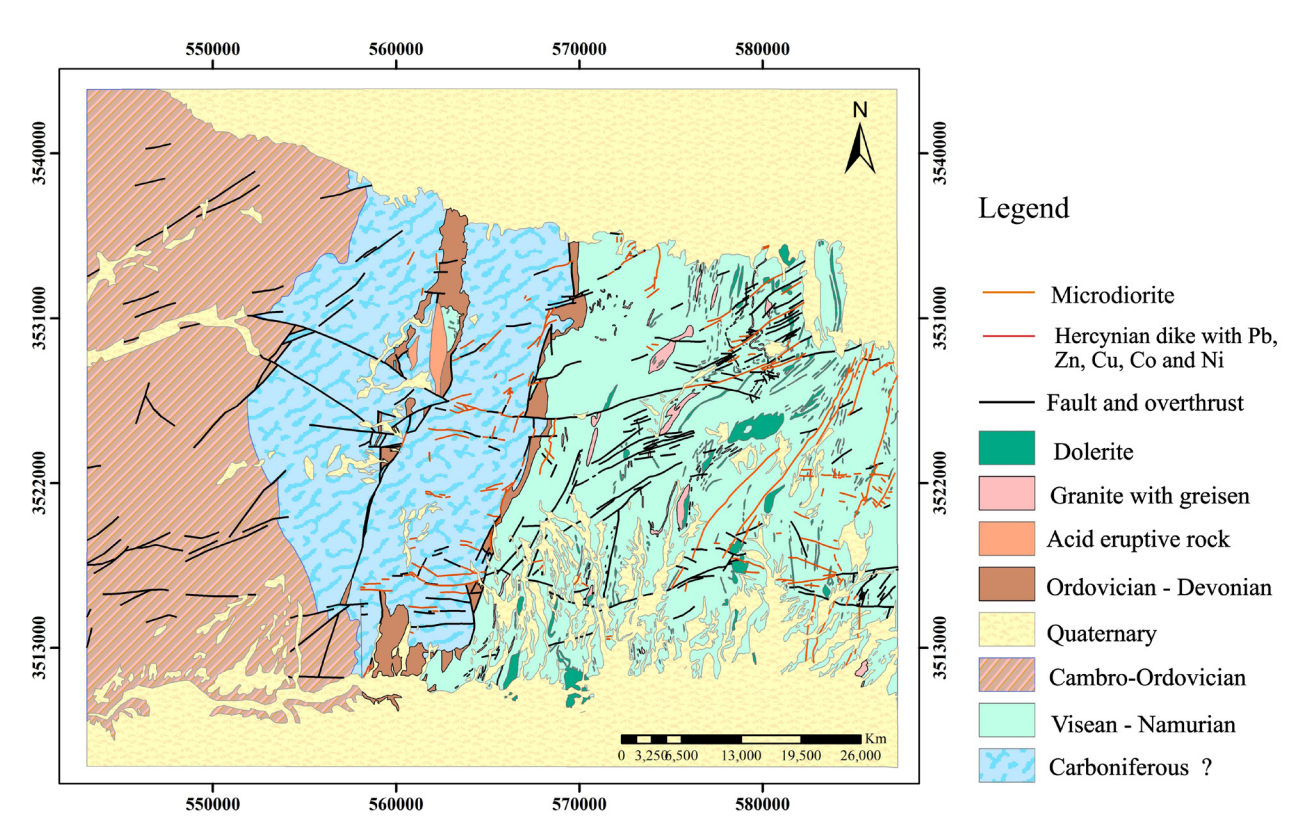


Fig. 2. Simplified geological and structural map of east-central Jebilet, 1:100,000 (Huvelin, 1977).

intrusions, including gabbros and microdiorites, associated with hydrothermal phenomena such as quartz veins and iron caps rich in iron oxides (Benharref & Schaer, 1991). These geological characteristics are particularly notable in the east-central parts of the Jebilet, where hydrothermal alterations and mineralisation linked to tectonics can be observed (Admou et al., 2018).

Geographically, the Jebilet extend approximately 60 km in length and 30 km in width, with an average altitude ranging between 400 and 800 metres (Fig. 1). The region is bordered to the south by the Haouz plain, an alluvial plain surrounding Marrakech, and to the north by the Plateau des Phosphates (Fig. 2; Huvelin, 1977). The approximate co-ordinates of the Jebilet are between 31°50′ and 32°00′ north latitude and 7°40′ and 8°00′ west longitude (Michard, 1976).

3. Material and methods

The Advanced Spaceborne Thermal Emission and Reflection Radiometer (ASTER) is a medium-high spatial resolution instrument that provides data in 14 spectral bands covering the visible through the thermal infrared wavelength region. A number of standard data products are available

to users through an on-line archival and processing system. Particular, user-specified data acquisitions are possible through a Data Acquisition Request system (Abrams, 2000). ASTER provides observations in three spectral regions and stereo observations using three separate radiometers (Table 1). The Visible and Near-Infrared (VNIR) system features three spectral bands ranging from 0.52 to 0.86 μm with a resolution of 15 metres; the Short-Wavelength Infrared (SWIR) subsystem includes six spectral bands from 1.60 to 2.45 μm with a resolution of 30 metres, and the Thermal Infrared (TIR) subsystem comprises five spectral bands spanning 8.125 to 11.65 μm , with a resolution of 90 metres.

The image used in the present work is an AS-TER that has undergone layer stacking of the SWIR and VNIR bands with ENVI 5.3 software, using the nearest neighbour algorithm to achieve a resolution of 15m. This method was chosen to preserve the spectral integrity of the data during resampling. The nearest neighbour interpolation minimises the risk of introducing spectral distortions, but its impact on spatial accuracy was assessed and found to be negligible for the purposes of the present study. An atmospheric correction using IAR Reflectance and a radiometric correction using Dark Object Subtraction were then applied to the VNIR-SWIR bands. Following these corrections, the ASTER im-

Table 1. ASTER instrument specifications (Abrams, 2000).

Wavelength region	Spatial resolu- tion (m)	Band	Spectral range (µm)
VNIR	15	1 2 3	0.52-0.60 0.63-0.69 0.76-0.86
SWIR	30	4 5 6 7 8 9	1.60-1.70 2.145-2.185 2.185-2.225 2.235-2.285 2.295-2.365 2.360-2.430
TIR	90	10 11 12 13 14	8.125-8.475 8.475-8.825 8.925-9.275 10.25-10.95 10.95-11.65

age was cropped to include only the study area. After the atmospheric correction, the reflectance imagery showed significant improvements in the spectral profiles of the minerals studied (Baid et al., 2023). After pre-processing the ASTER images, we applied various techniques including image noise reduction, RGB combinations, band ratios, PCA and MNF transformations, with band ratio classification as outlined in Baid et al. (2023). The GIS layers were prepared using ArcGIS 10.8 software. The accuracy of the results from the two sensors was validated against the 1:100,000 geological map by Huvelin (1977). A detailed overview of the methodology is presented in Figure 3.

After pre-processing the ASTER images, several image processing techniques were applied, including noise reduction, RGB combinations, principal component analysis (PCA), minimum noise frac-

tion (MNF) and, particularly, band ratio classifications as outlined in Baid et al. (2023).

Principal Component Analysis (PCA) was applied to the corrected ASTER VNIR and SWIR bands in order to reduce spectral redundancy and enhance the discrimination of lithological units. This method transforms the original bands into new uncorrelated components by maximising the variance of spectral information (Hung et al., 2005). Several RGB combinations of the first three principal components (PC1, PC2, PC3) were tested to optimise the visualisation of lithological contrasts, as recommended by Amer et al. (2012). The MNF is particularly effective in separating useful signals from artifacts and noise, making it a valuable tool for material identification and geological mapping (Green et al., 1988). This technique is especially beneficial in studies where hyperspectral data are affected by factors such as atmospheric variability or illumination conditions, and where efficient noise reduction is crucial for accurate results (Boardman, 1993).

In the present study, specific band ratios were selected based on their proven effectiveness in previous mineralogical and lithological mapping studies (Zhang et al., 2016; Testa et al., 2018; Salehi et al., 2019; Abdelouhed et al., 2021; Baid et al., 2023). These ratios highlight the spectral signatures of diagnostic minerals while reducing the effects of topographic shading. For example, (b7/b5) was used to detect kaolinite; (b4 + b6)/b5 for iron oxides and alteration minerals originated in an acidic environment; ((b7 + b9)/b8) for carbonates, chlorite and epidote; ((b6 + b9)/(b7 + b8)) for endoskarn assemblages; ((b5 + b7)/b6) for phyllic alteration (sericite, illite, muscovite); and (b5/b6) for phengite(Hewson

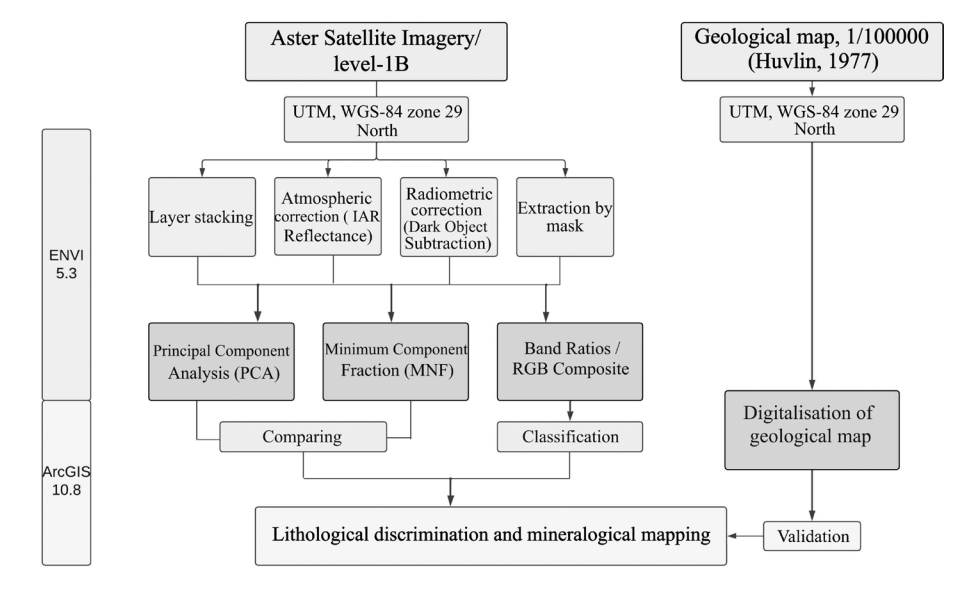


Fig. 3. Methodology flow-chart.

et al., 2005). These band ratios were applied to the corrected ASTER image so as to generate maps of mineral distribution reflecting the lithological variability of the study area.

To validate and refine the results derived from satellite image interpretation, a field survey was carried out. According to the regional geological context described by Huvelin (1977), the area consists of Cambrian-Ordovician metasedimentary rocks, Visean-Namurian formations and Carboniferous volcano-sedimentary units. During field observations, the main lithological contacts and alteration zones, as identified through remote sensing, were inspected and sampled. The presence of minerals such as kaolinite, sericite, epidote and chlorite was confirmed in outcrops that corresponded to spectral anomalies. This validation step was essential to confirm that the spectral responses and maps accurately represent the mineralogical and lithological features of the region.

4. Results

4.1. Band ratios (BR)

Through the analysis of ASTER spectral bands, the mineralogical composition of the study area was mapped, revealing the presence of several key minerals. For instance, the band ratio (band7/band5) effectively mapped the distribution of kaolinite (Fig. 4), which is abundant in the northern and central parts of the study area, associated with Visean-Namurian-aged formations. Similarly, the ratio (band4+band6/band5) highlighted the presence of minerals such as alunite, kaolinite and pyrophyllite, particularly in the northern and southern regions, as well as in the west, corresponding to Cambrian-Ordovician terrains.

The ratio ((band7+band9)/band8) mapped minerals such as carbonate, chlorite and epidote, while the ratio ((band6+band9)/(band7+band8)) was used to map endoskarns consisting of epidote, chlorite and amphibole (Fig. 4), showing similar distributions in the Visean-Namurian and Carboniferous terrains. Furthermore, the ratio ((band5+band7)/band6) was used to identify phyllic alteration, with minerals such as sericite, muscovite, illite and smectite being highly concentrated in the western parts of the region, specifically in Cambrian-Ordovician and Carboniferous strata (Fig. 4).

In addition, the presence of phengite was mapped using the band ratio (band5/band6), re-

vealing its moderate abundance in the Cambrian-Ordovician and Carboniferous terrains.

4.2. Principal component analysis (PCA)

The application of principal component analysis (PCA) to the corrected ASTER VNIR and SWIR bands enabled a clear differentiation of lithological units throughout the study area. RGB combinations of the first three principal components (PC1, PC2, PC3) were tested, and the combination PC1 (band 1), PC2 (band 2) and PC3 (band 3) was found to provide the best visual contrast for interpreting geological variations (Hung et al., 2005; Amer et al., 2012). In the present study, this combination proved to be the most effective (Fig. 5), allowing for the clear distinction of lithological units corresponding to different geological ages based on their spectral signatures. It allows for the differentiation of rocks with various geological ages, where Carboniferous (C) and Visean-Namurian (V-B) rocks (Huvelin, 1977) exhibit blue and violet hues, visible in the central and eastern parts. A second distinction, with a light pink to slightly orange hue, corresponds to Ordovician and Devonian rocks (O-D; Huvelin, 1977) in the central part of the area. The light blue hue in the west characterises Cambrian-Ordovician rocks (€-O; Huvelin, 1977), while the green and dark pink hues represent Quaternary formations (Q; Huvelin, 1977), visible in the northern and southern parts of the study area.

4.3. Minimum noise fraction (MNF)

MNF is a technique used in hyperspectral data analysis to enhance the signal-to-noise ratio by reducing noise and improving data quality before further processing. Introduced by Green et al. (1988) and Zhang et al. (2016), this method involves a twostep linear transformation: the first step minimises noise in the data, while the second applies a principal component analysis to order the pixels based on their spectral quality. The MNF results from ASTER data can be visually evaluated (Fig. 6). The initial MNF bands capture the signals, whereas the subsequent bands predominantly contain noise. The Ordovician and Devonian (O-D) formations appear in light grey on the MNF map, while the Carboniferous (C) and Visean-Namurian (V-B) rocks are represented in dark brown. The Cambrian-Ordovician (€-O) rocks are shown in light brown to greyish tones, and the Quaternary sediments (Q) are also clearly visible in the south and appear to some ex-

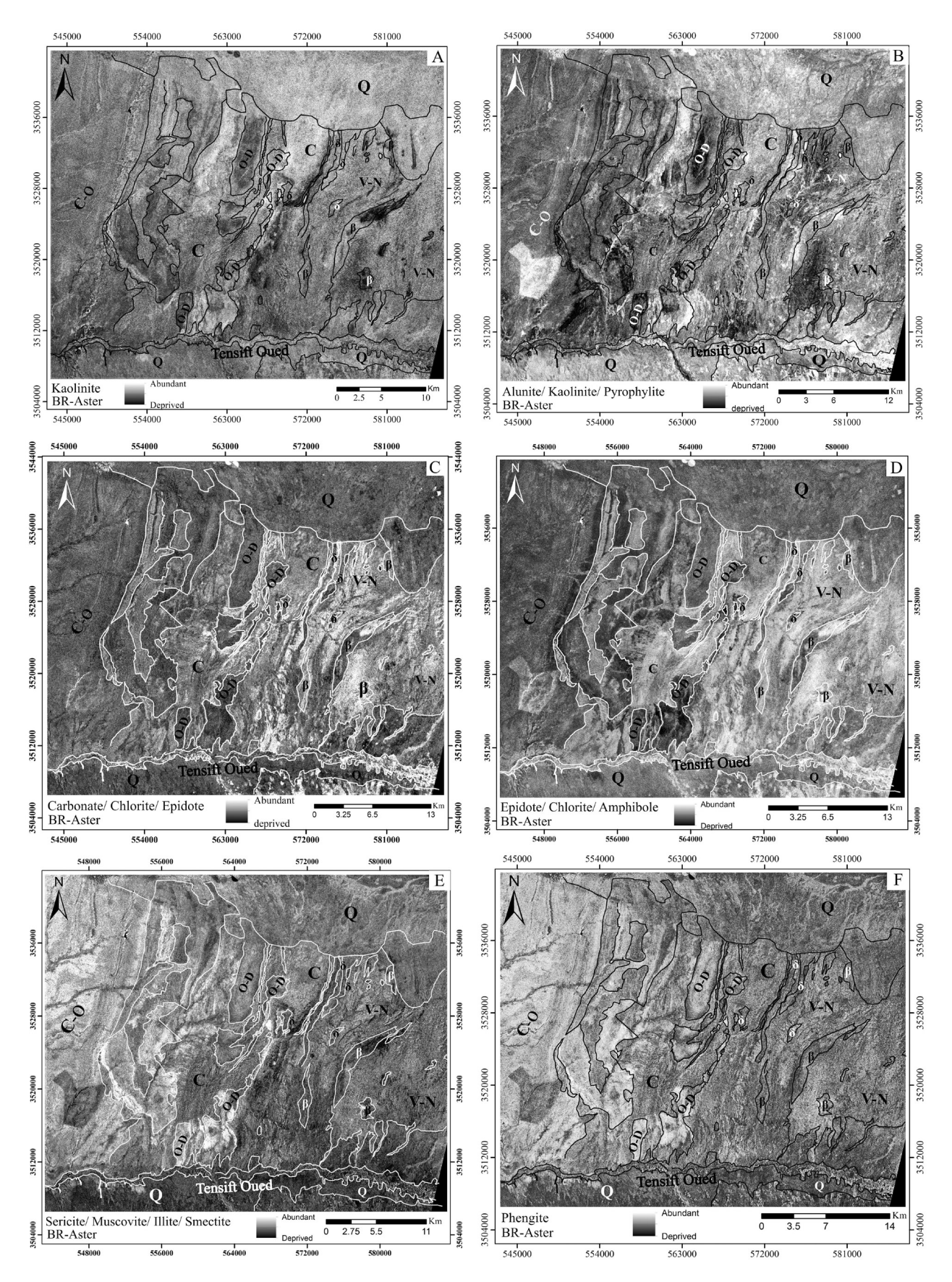


Fig. 4. BR of ASTER sensor. **A** – Kaolinite; **B** – Alunite-kaolinite-pyrophyllite; **C** – Carbonate-chlorite-epidote; **D** – Epidote-chlorite-amphibole; **E** – Sericite-muscovite-illite-smectite; **F** – Phengite.

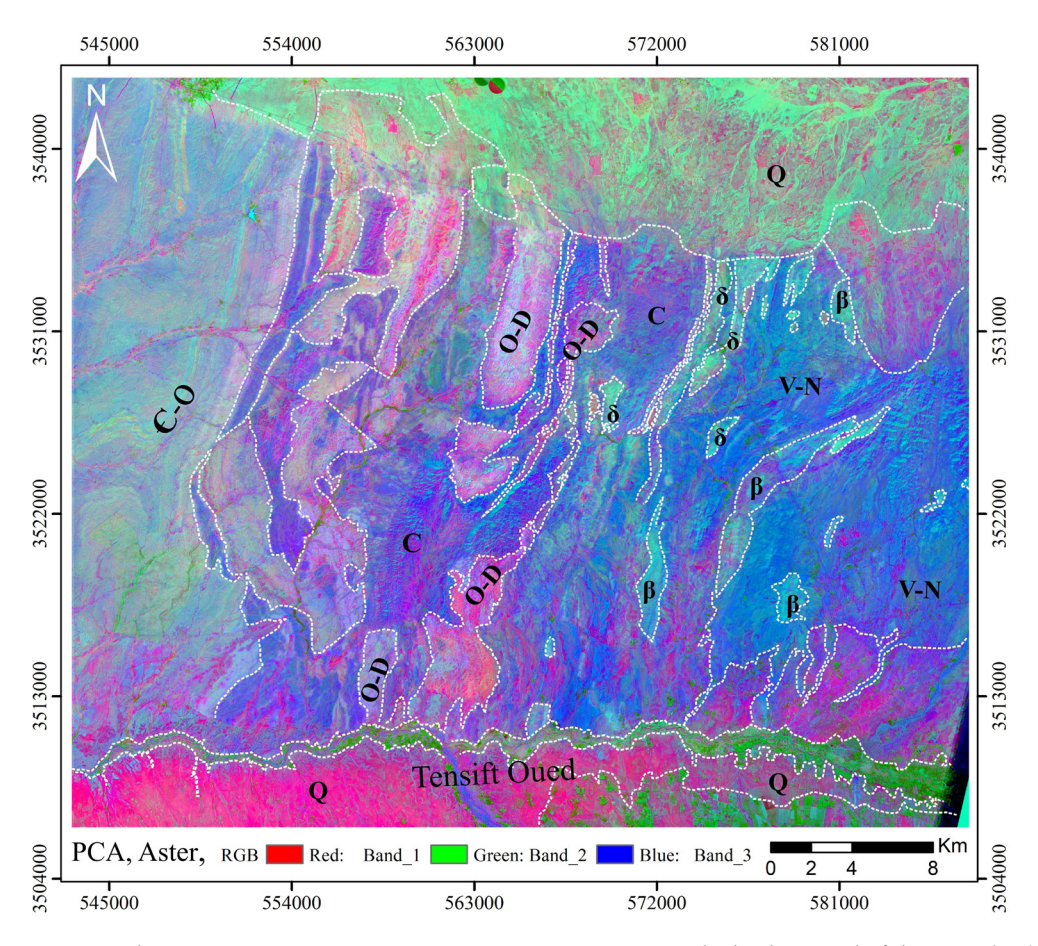


Fig. 5. PCA1, PCA2 and PCA3 images ASTER as an RGB composite, against the background of the Huvelin (1977) map. C – Carboniferous, V-N – Visean-Namurian, O-D – Ordovician-Devonian; ε -O – Cambro-Ordovician, Q – Quaternary, β – basic intrusion (dolerite), δ – acidic intrusion (granite with greisen).

tent in the north. The MNF processing has provided excellent discrimination of the lithologies within our study area, allowing for clear identification of the different formations.

5. Discussion

In the east-central Jebilet region, ASTER images were utilised after undergoing atmospheric, radiometric and reflectance corrections to produce mineral alteration maps. The applied processes, such as colour composition, band ratios, principal component analysis (PCA) and minimum noise fraction (MNF), enabled precise lithological discrimination and the extraction of mineral alteration maps, as illustrated in Figures 4, 5 and 6. Remote sensing techniques, particularly effective for mapping lithological units in mountainous areas, proved especially useful in the region studied. The comparison of the results of transformation methods, such as PCA and MNF, validated the occurrence of geological formations by cross-referencing the results from

ASTER images with the geological map of Huvelin (1977). This approach clearly identified lithological boundaries and assigned distinct colours to each unit. Potential sources of error in the present study stem primarily from sensor limitations, data processing choices and spectral ambiguity. First, the spatial resolution of ASTER's SWIR bands (30 m) and TIR bands (90 m) may result in spectral mixing, especially in heterogeneous terrains like the Jebilet region, where lithologies are closely interbedded. This mixing can reduce the accuracy of mineral identification, particularly for narrow or discontinuous units (Hosseinjani & Tangestani, 2011; van der Meer et al., 2012; Zhang et al., 2016). Secondly, the resampling of SWIR bands to match the VNIR resolution (15 m) using the nearest neighbour method, while preserving spectral fidelity, may still introduce spatial distortion or edge effects (Jensen, 2009). Thirdly, the atmospheric correction, although applied, depends heavily on model assumptions and the presence of reference targets, which may not always be uniformly distributed across the scene (Chavez, 1996). Additionally, the use of band ratios

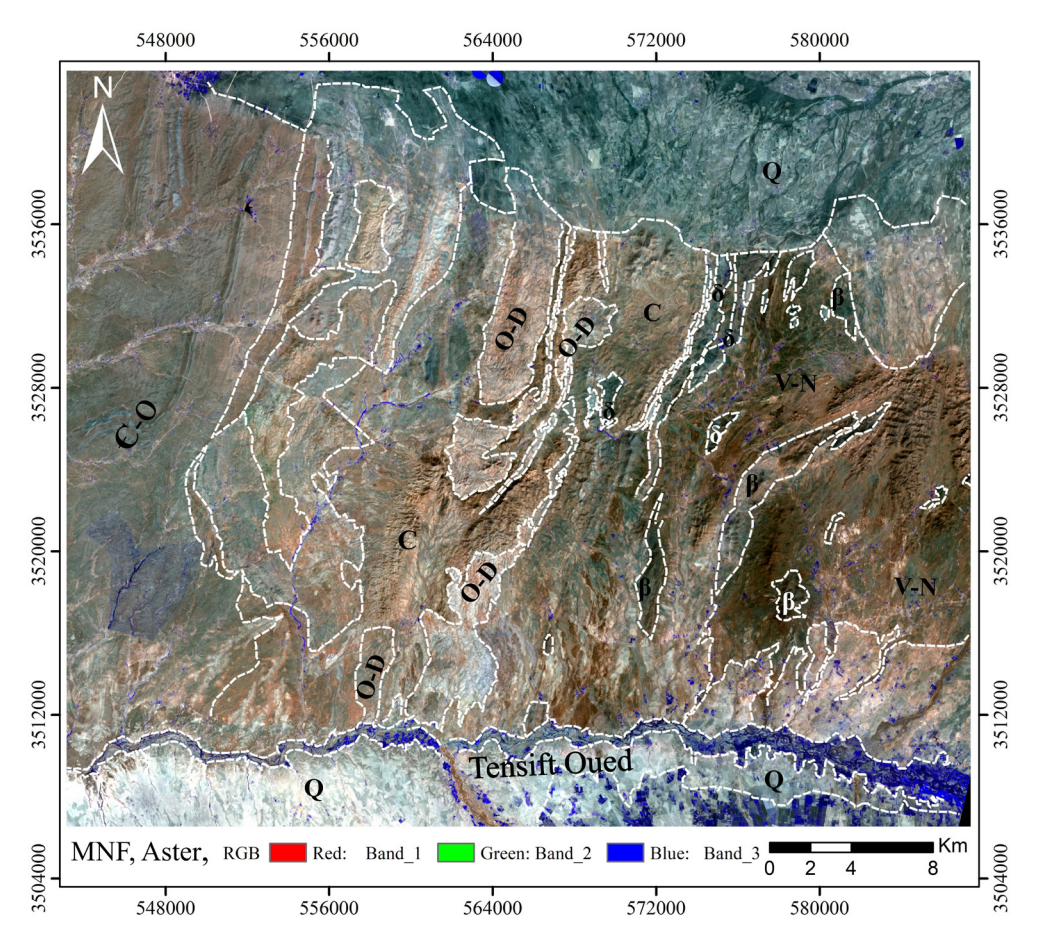


Fig. 6. MNF1, MNF2 and MNF3 images ASTER as an RGB composite, against the background of the Huvelin (1977) map. C – Carboniferous, V-N – Visean-Namurian, O-D – Ordovician-Devonian, ε -O – Cambro-Ordovician, Q – Quaternary, β – basic intrusion (dolerite), δ – acidic intrusion (granite with greisen).

and principal component analysis assumes consistent illumination and surface conditions, which may not hold due to topographic shadowing and vegetation cover in some parts of the study area (Chabrillat et al., 2002). Finally, mineralogical ambiguities may arise when distinct minerals exhibit similar spectral responses in the VNIR-SWIR range, potentially leading to misclassification (Clark et al., 2007; van der Meer et al., 2012). Despite these limitations, field verification and comparison with the 1:100,000 geological map by Huvelin (1977) served as important validation tools in assessing and mitigating these uncertainties.

The two sensors demonstrated complementarity, yielding nearly identical outcomes. Several studies have previously employed various methods for distinguishing and mapping surface rock types using multispectral data, including band ratios (BR), principal component analysis (PCA) and minimum noise fraction (MNF) (Yamaguchi & Naito, 2003; Abdelouhed et al., 2021; Ouhoussa et al., 2023). These approaches, particularly the use of band ratios, enhance spectral differences and minimise the

impact of topographic shading (Abdelouhed et al., 2021). However, as demonstrated in the present study, combining multiple spectral bands allows for a more detailed and effective lithological and mineralogical mapping in the area.

The band ratios (BR) applied in the present study effectively highlighted several groups of minerals, such as kaolinite, alunite and pyrophyllite, or a carbonate mineral, chlorite and epidote. However, the detection of certain minerals, such as phengite, was limited due to spectral band overlap and resolution constraints. These limitations are likely linked to ASTER's spatial resolution and the spectral similarity of some minerals, underscoring the need for field validation and, where possible, the use of higher-resolution or complementary datasets.

Although remote sensing techniques have been widely applied in various geological contexts, the study by Abdelouhed et al. (2021) focused specifically on mapping hydrothermal alteration zones in the same study area. They used the same ASTER band ratios to detect Al-OH bearing minerals such as alunite, muscovite, kaolinite and illite. These al-

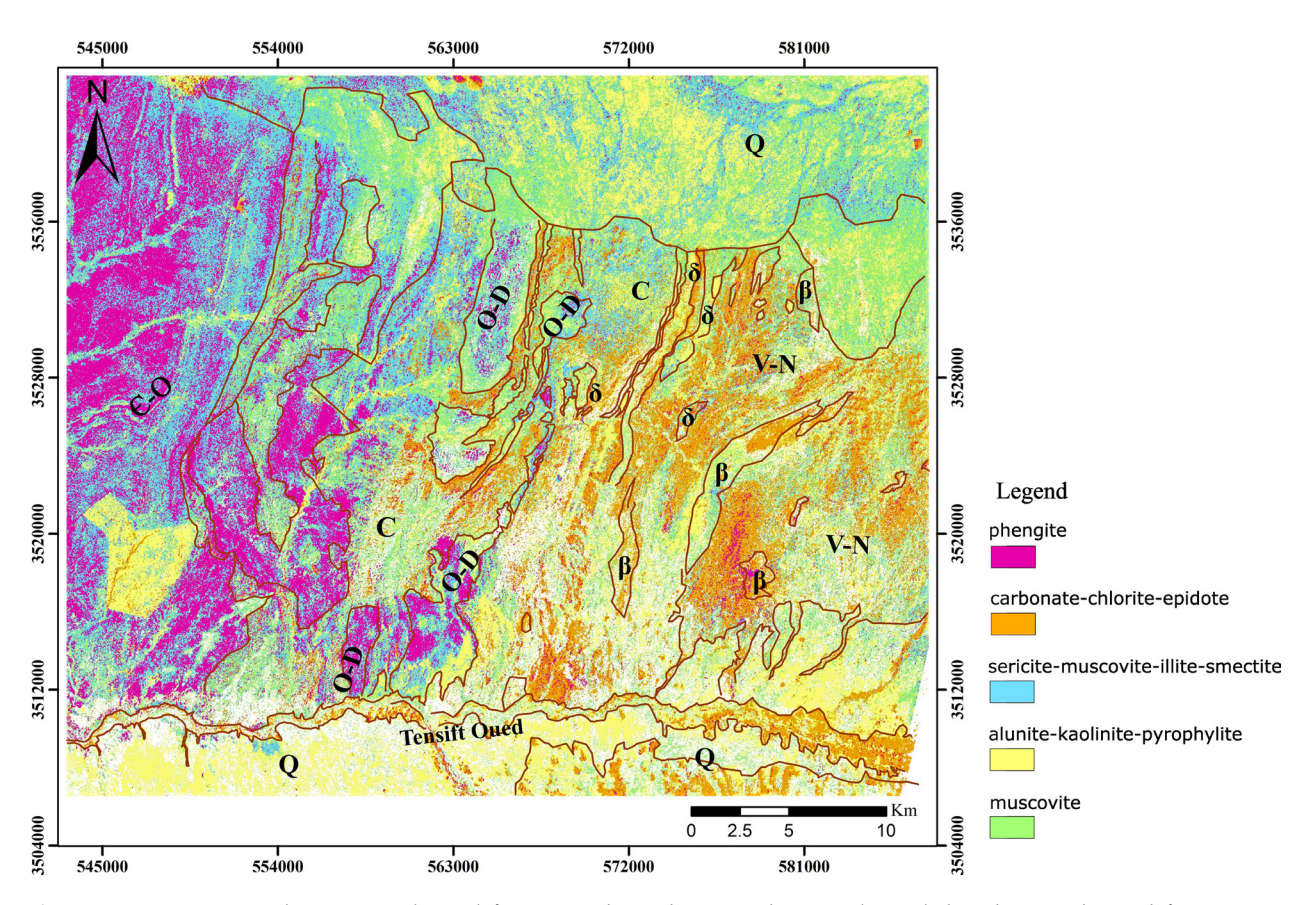


Fig. 7. Overview map showing geological formation boundaries and mineralogical distribution derived from PCA, MNF and classified BR results of ASTER imagery.

teration minerals were effectively identified using ASTER's SWIR and VNIR bands. Our study confirms and extends these findings by showing that these minerals, along with chlorite and phengite, are also useful indicators for broader lithological differentiation in the Jebilet region.

Figure 7 demonstrates a classification of all band ratios to pinpoint areas abundant in the identified minerals. This involved overlaying principal components (PCA1, PCA2, PCA3) and minimum noise fractions (MNF1, MNF2, MNF3) derived from the ASTER images. The PCA and MNF transformations were performed to enhance spectral contrast and reduce noise, enabling a clearer distinction of mineralogical and lithological features. The RGB combinations, such as PCA1-PCA4-PCA3 and MNF1-MNF4-MNF3, were particularly effective in enhancing the visual discrimination of Palaeozoic lithological formations.

To validate the results obtained from the images and spatial maps, we conducted several direct field observations. Figure 8 illustrates various sandstones and shale containing clay minerals. These images correspond closely with the mineral assemblages and lithological structures identified

through ASTER image analysis. Furthermore, the remote sensing interpretation was cross-checked with the geological map by Huvelin (1977), which further supports the reliability of the mapped lithological boundaries and mineral zones. This integration of remote sensing, image processing and field verification reinforces the robustness of the proposed methodology for lithological and mineralogical mapping in the east-central Jebilet region.

6. Conclusions

The present study demonstrates the potential of ASTER multispectral data, combined with image processing techniques such as band ratios, PCA and MNF, to support lithological and mineralogical mapping in the east-central Jebilet region. The integration of remote sensing data with field observations and comparison with the geological map of Huvelin (1977) contributed to the identification of distinct lithological units and areas of mineral alteration. While some limitations remain, particularly in terms of spatial resolution and spectral similarity, this approach proved useful for improving ge-

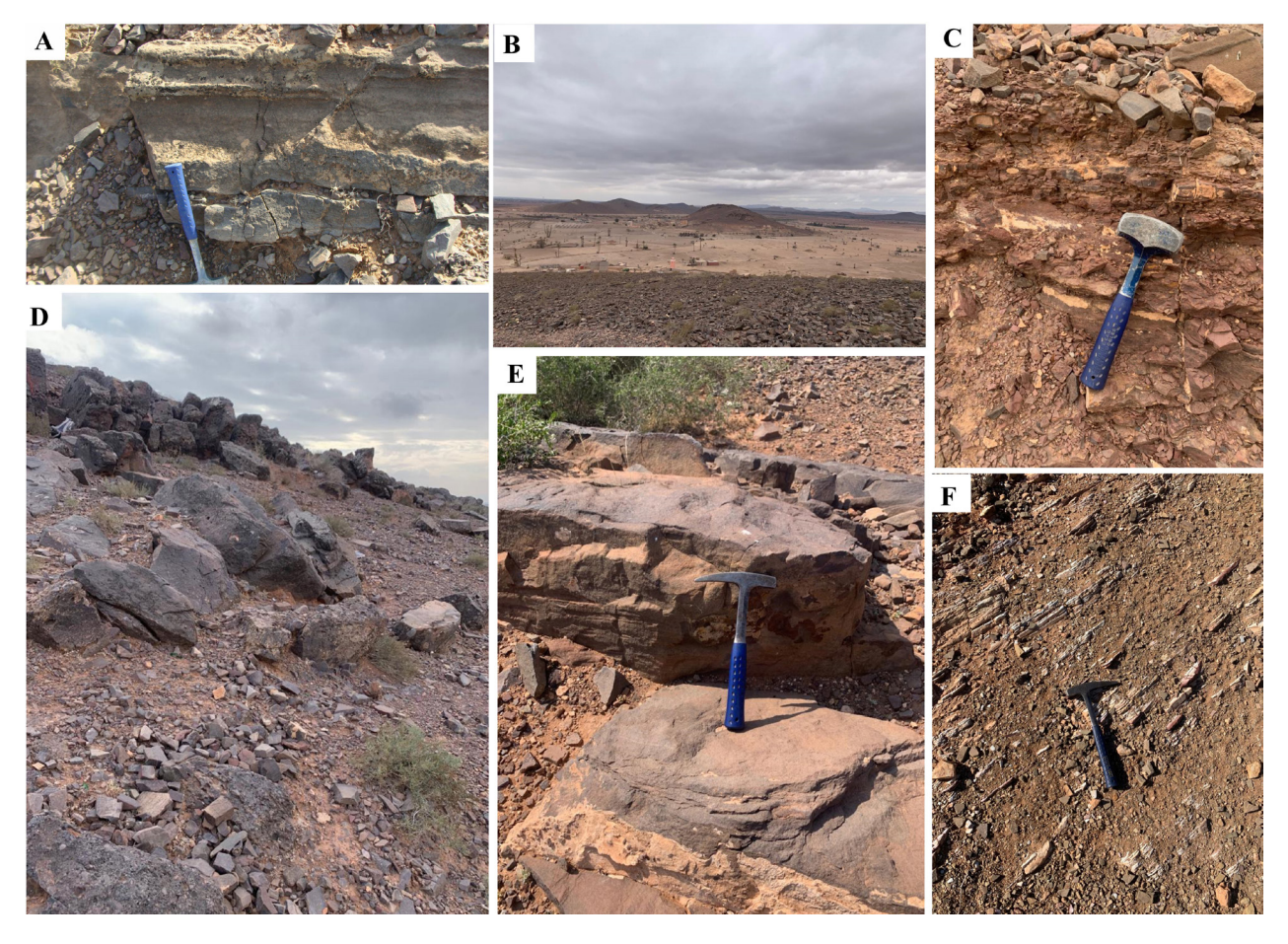


Fig. 8. Rocks of the east-central Jebilet region. A – Sandstone; B – Panoramic view of the entire eastern Jebilet; C – Sandstone outcrop; D – Conglomerate and sandstone; E – Fractured block of sandstone; F – Pelite composed of clay minerals such as illite and kaolinite.

ological interpretation in complex terrains. Future studies using higher-resolution or hyperspectral data could further refine these results and address the remaining ambiguities.

Acknowledgements

The authors express their sincere thanks to the Department of Geology and Geosciences, Geotourism, Natural Hazards and Remote Sensing Laboratory at Cadi Ayyad University for their support throughout this study. We deeply appreciate comments, suggestions and corrections of both anonymous reviewers.

References

Abdelouhed F., Algouti A., Algouti A., Mohammed I. & Mourabit Z., 2021. Contribution of GIS and remote sensing in geological mapping, lineament extractions and hydrothermal alteration minerals mapping us-

ing ASTER satellite images: case study of central Jebilets-Morocco. *Disaster Adv*ances 14, 15–25.

Abrams M., 2000. The Advanced Spaceborne Thermal Emission and Reflection Radiometer (ASTER): data products for the high spatial resolution imager on NASA's Terra platform. *International Journal of Remote Sensing* 21, 847–859.

Admou S., Branquet Y., Badra L., Barbanson L., Outhounjite M., Khalifa A., Zouhair M. & Maacha L., 2018. The hajjar regional transpressive shear zone (Guemassa massif, Morocco): consequences on the deformation of the base-metal massive sulfide ore. *Minerals* 8, 435.

Amer R., Kusky T. & El Mezayen A., 2012. Remote sensing detection of gold related alteration zones in Um Rus area, Central Eastern Desert of Egypt. Advances in Space Research 49, 121–134.

Baid S., Tabit A., Algouti A., Algouti A., Nafouri I., Souddi S., Aboulfaraj A., Ezzahzi S. & Elghouat A., 2023. Lithological discrimination and mineralogical mapping using Landsat-8 OLI and ASTER remote sensing data: Igoudrane region, jbel saghro, Anti Atlas, Morocco. Heliyon 9.

Boardman J.W., 1993. Automating spectral unmixing of AVIRIS data using convex geometry concepts. *Sum*-

- maries of the 4th Annual JPL Airborne Geoscience Workshop. Vol. 1, JPL Publication 93–26, pp. 11–14.
- Bouloton J., Gasquet D. & Pin C., 2019. Petrogenesis of the Early-Triassic quartz-monzodiorite dykes from Central Jebilet (Moroccan Meseta): Trace element and Nd-Sr isotope constraints on magma sources, and inferences on their geodynamic context. *Journal of African Earth Sciences* 149, 451–464.
- Brimhall G.H., Dilles J.H. & Proffett J.M., 2005. *The role of geologic mapping in mineral exploration*. [In:] M.D. Doggett & J.R. Parry (Eds): Wealth creation in the minerals industry: Integrating science, business, and education. Spec. Publ. 12, pp. 221–241.
- Chen W., Li X., Qin X. & Wang L., 2024. Geological Remote Sensing: An overview BT Remote sensing intelligent interpretation for geology: From perspective of geological exploration. [In:] W. Chen, X. Li, X. Qin & L. Wang (Eds): Remote sensing intelligent interpretation for geology: From perspective of geological exploration, pp. 1–14, Springer Nature Singapore. https://doi.org/10.1007/978-981-99-8997-3_1
- Green A.A., Berman M., Switzer P. & Craig M.D., 1988. A transformation for ordering multispectral data in terms of image quality with implications for noise removal. *IEEE Transactions on Geoscience and Remote Sensing* 26, 65–74.
- Guanter L., Kaufmann H., Segl K., Foerster S., Rogass C., Chabrillat S., Kuester T., Hollstein A., Rossner G. & Chlebek C., 2015. The EnMAP spaceborne imaging spectroscopy mission for earth observation. *Remote Sensing* 7, 8830–8857.
- Hewson R.D., Cudahy T.J., Mizuhiko S., Ueda K. & Mauger A.J., 2005. Seamless geological map generation using ASTER in the Broken Hill-Curnamona province of Australia. *Remote Sensing of Environment* 99, 159–172.
- Hung L.Q., Batelaan O. & De Smedt F., 2005. Lineament extraction and analysis, comparison of LANDSAT ETM and ASTER imagery. Case study: Suoimuoi tropical karst catchment, Vietnam. Remote Sensing for Environmental Monitoring, GIS Applications, and Geology V, 5983, 182–193.
- Huvelin P., 1977. Etude geologique et gitologique du massif hercynien des Jebilet (Maroc occidental). Notes et Mé-

- moires du Service Géologique du Maroc, 232 bis, 308 pp.
- Laurent D.L.H., 2019. *Identification des sites de minéralisation par l'imagerie satellite dans le Hoggar, région d'Issalane (Tazrouk, Algérie)*. Université Abou Bekr Belkaid – Tlemcen, 108 pp.
- Mahdevar M., Ketabi P., Saadatkhah N. & Rahnamarad J., 2014. Application of ASTER SWIR data on detection of alteration zone in the Sheikhabad area, eastern Iran. *Arabian Journal of Geosciences* 8. https://doi.org/10.1007/s12517-014-1597-2
- Michard A., 1976. *Eléments de géologie marocaine*. Notes and Memoirs of the Geological Survey of Morocco, 252, 408 pp.
- Ouhoussa L., Ghafiri A., Aissi L. Ben & Es-Sabbar B., 2023. Integrating aster images processing and fieldwork for identification of hydrothermal alteration zones at the oumjrane-boukerzia district, Moroccan Anti-Atlas. *Open Journal of Geology* 13, 171–188.
- Salehi S., Mielke C., Brogaard Pedersen C. & Dalsenni Olsen S., 2019. Comparison of ASTER and Sentinel-2 spaceborne datasets for geological mapping: a case study from North-East Greenland. *Geological Survey of Denmark and Greenland Bulletin* 43, 1–6. https://doi.org/10.34194/geusb.v43.4305
- Testa F.J., Villanueva C., Cooke D.R. & Zhang L., 2018. Lithological and hydrothermal alteration mapping of epithermal, porphyry and tourmaline breccia districts in the Argentine Andes using ASTER imagery. *Remote Sensing* 10, 203.
- Yamaguchi Y. & Naito C., 2003. Spectral indices for lithologic discrimination and mapping by using the AS-TER SWIR bands. *International Journal of Remote Sensing* 24, 4311–4323.
- Zhang T., Yi G., Li H., Wang Z., Tang J., Zhong K., Li Y., Wang Q. & Bie X., 2016. Integrating data of ASTER and Landsat-8 OLI (AO) for hydrothermal alteration mineral mapping in Duolong porphyry Cu-Au deposit, Tibetan Plateau, China. *Remote Sensing* 8, 890.

Manuscript submitted: 20 December 2024 Revision accepted: 15 May 2025